First-principles calculations of hot-electron lifetimes in metals

I. Campillo
Materia Kondentsatuaren Fisika Saila, Zientzi Fakultatea, Euskal Herriko Unibertsitatea, 644 Posta kutxatila, 48080 Bilbo, Basque Country, Spain

V. M. Silkin
Materialen Fisika Saila, Kimika Fakultatea, Euskal Herriko Unibertsitatea, 1072 Posta kutxatila, 20080 Donostia, Basque Country, Spain

J. M. Pitarke
Materia Kondentsatuaren Fisika Saila, Zientzi Fakultatea, Euskal Herriko Unibertsitatea, 644 Posta kutxatila, 48080 Bilbo, Basque Country, Spain
and Donostia International Physics Center (DIPC) and Centro Mixto CSIC-UPV/EHU, Donostia, Spain

E. V. Chulkov
Materialen Fisika Saila, Kimika Fakultatea, Euskal Herriko Unibertsitatea, 1072 Posta kutxatila, 20080 Donostia, Basque Country, Spain
and Donostia International Physics Center (DIPC) and Centro Mixto CSIC-UPV/EHU, Donostia, Spain

A. Rubio
Departamento de Física Teórica, Universidad de Valladolid, 47011 Valladolid, Spain

P. M. Echenique
Materialen Fisika Saila, Kimika Fakultatea, Euskal Herriko Unibertsitatea, 1072 Posta kutxatila, 20080 Donostia, Basque Country, Spain
and Donostia International Physics Center (DIPC) and Centro Mixto CSIC-UPV/EHU, Donostia, Spain
(Received 3 November 1999)

First-principles calculations of the inelastic lifetime of low-energy electrons in Al, Mg, Be, and Cu are reported. Quasiparticle damping rates are evaluated from the knowledge of the electron self-energy, which we compute within the *GW* approximation of many-body theory. Inelastic lifetimes are then obtained along various directions of the electron wave vector, with full inclusion of the band structure of the solid. Average lifetimes are also reported, as a function of the electron energy. In Al and Mg, splitting of the band structure over the Fermi level yields electron lifetimes that are smaller than those of electrons in a free-electron gas. Larger lifetimes are found in Be, as a result of the characteristic dip that this material presents in the density of states near the Fermi level. In Cu, a major contribution from *d* electrons participating in the screening of electron-electron interactions yields electron lifetimes that are well above those of electrons in a free-electron gas with the electron density equal to that of valence $(4s^1)$ electrons.

I. INTRODUCTION

Low-energy excited electrons in metals, with energies larger than ~ 0.5 eV above the Fermi energy, experience strong electron-electron $(e\text{-}e)$ scattering processes. Although inelastic lifetimes of these so-called hot electrons have been investigated for many years on the basis of the free-electron-gas (FEG) model of the solid,[1–10] time-resolved two-photon photoemission (TR-2PPE) experiments have shown the key role that band-structure effects may play in the decay mechanism.[11–20] First-principles calculations of hot-electron lifetimes that fully include the band structure of the solid have been reported only very recently for aluminum and copper.[21,22] These calculations[21] show that actual lifetimes are the result of a delicate balance between localization, density of states, screening, and Fermi-surface topology, even in the case of a free-electron-like metal such as aluminum.

In this paper, we report first-principles calculations of inelastic lifetimes of excited electrons in a variety of real metals. We start with free-electron-like trivalent (Al) and divalent (Mg) metals, and then focus on divalent Be and the role that *d* electrons play in a noble metal like Cu. First, we expand the one-electron Bloch states in a plane-wave basis, and solve the Kohn-Sham equation of density-functional theory[23] (DFT) by invoking the local-density approximation (LDA) for exchange and correlation (XC). The electron-ion interaction is described by means of nonlocal, norm-conserving ionic pseudopotentials, and we use the one-electron Bloch states to evaluate the screened Coulomb interaction in the random-phase approximation (RPA).[24] We finally evaluate the lifetime of an excited Bloch state from the knowledge of the imaginary part of the electron self-energy, which we compute within the *GW* approximation of many-body theory.[25] Our calculations indicate that scattering

rates may strongly depend, for a given electron energy, on the direction of the wave vector of the initial state. Also, average lifetimes, as obtained by averaging over all wave vectors and bands with the same energy, are found to deviate considerably from those derived for a FEG.

The rest of this paper is organized as follows: Explicit expressions for the electron decay rate in periodic crystals are derived in Sec. II, within the GW approximation of many-body theory. Calculated inelastic lifetimes of hot electrons in Al, Mg, Be, and Cu are presented in Sec. III, and the conclusions are given in Sec. IV. Atomic units are used throughout, i.e., $e^2=\hbar=m_e=1$.

II. THEORY

Take an inhomogeneous electron system. In the framework of many-body theory,[24] the damping rate τ_i^{-1} of an excited electron in the state $\phi_i(\mathbf{r})$ with energy E_i is obtained from the knowledge of the imaginary part of the electron self-energy, $\Sigma(\mathbf{r},\mathbf{r}';E_i)$, as

$$\tau_i^{-1}=-2\int d\mathbf{r}\int d\mathbf{r}'\,\phi_i^*(\mathbf{r})\,\mathrm{Im}\,\Sigma(\mathbf{r},\mathbf{r}';E_i)\,\phi_i(\mathbf{r}'). \quad (1)$$

In the GW approximation,[25] one considers only the first-order term in a series expansion of the self-energy in terms of the screened Coulomb interaction:

$$\Sigma(\mathbf{r},\mathbf{r}';E_i)=\frac{i}{2\pi}\int dE\,G(\mathbf{r},\mathbf{r}';E_i-E)\,W(\mathbf{r},\mathbf{r}';E), \quad (2)$$

where $G(\mathbf{r},\mathbf{r}';E_i-E)$ represents the one-particle Green function and $W(\mathbf{r},\mathbf{r}';E)$ is the time-ordered screened Coulomb interaction. After replacing the Green function (G) by the zero-order approximation (G^0), the imaginary part of the self-energy can be evaluated explicitly:

$$\mathrm{Im}\,\Sigma(\mathbf{r},\mathbf{r}';E_i)=\sum_f\,\phi_f^*(\mathbf{r}')\,\mathrm{Im}\,W(\mathbf{r},\mathbf{r}';\omega)\,\phi_f(\mathbf{r}), \quad (3)$$

where $\omega=E_i-E_f$ represents the energy transfer, the sum is extended over a complete set of final states $\phi_f(\mathbf{r})$ with energy E_f ($E_F\leqslant E_f\leqslant E_i$), E_F is the Fermi energy, and

$$W(\mathbf{r},\mathbf{r}';\omega)=v(\mathbf{r}-\mathbf{r}')+\int d\mathbf{r}_1\int d\mathbf{r}_2 v(\mathbf{r}-\mathbf{r}_1)\times\chi(\mathbf{r}_1,\mathbf{r}_2;\omega)v(\mathbf{r}_2-\mathbf{r}'). \quad (4)$$

Here, $v(\mathbf{r}-\mathbf{r}')$ represents the bare Coulomb interaction, and $\chi(\mathbf{r},\mathbf{r}';\omega)$ is the density-density correlation function of the solid.

In the framework of time-dependent density-functional theory,[26,27] the density-density correlation function satisfies the integral equation

$$\chi(\mathbf{r},\mathbf{r}';\omega)=\chi^0(\mathbf{r},\mathbf{r}';\omega)+\int d\mathbf{r}_1\int d\mathbf{r}_2\chi^0(\mathbf{r},\mathbf{r}_1;\omega)\times[v(\mathbf{r}_1-\mathbf{r}_2)+K^{xc}(\mathbf{r}_1,\mathbf{r}_2;\omega)]\chi(\mathbf{r}_2,\mathbf{r}';\omega), \quad (5)$$

where $\chi^0(\mathbf{r},\mathbf{r}';\omega)$ is the density-density correlation function of noninteracting Kohn-Sham electrons, as described by the solutions of the time-dependent counterpart of the Kohn-Sham equation. In usual practice, these amplitudes are approximated by standard LDA wave functions. The kernel $K^{xc}(\mathbf{r}_1,\mathbf{r}_2;\omega)$, which accounts for the reduction in the e-e interaction due to the existence of short-range XC effects, is obtained from the knowledge of the XC energy functional. In the RPA, this kernel is taken to be zero.

For periodic crystals, one may introduce the following Fourier expansion for the screened interaction of Eq. (4):

$$W(\mathbf{r},\mathbf{r}';\omega)=\frac{1}{\Omega}\sum_{\mathbf{q}}^{\mathrm{BZ}}\sum_{\mathbf{G},\mathbf{G}'}e^{i(\mathbf{q}+\mathbf{G})\cdot\mathbf{r}}e^{-i(\mathbf{q}+\mathbf{G}')\cdot\mathbf{r}'}\times v_{\mathbf{G}}(\mathbf{q})\epsilon^{-1}_{\mathbf{G},\mathbf{G}'}(\mathbf{q},\omega), \quad (6)$$

where the first sum is extended over the first Brillouin zone (BZ), $\mathbf{G}$ and $\mathbf{G}'$ are reciprocal lattice vectors, Ω is the normalization volume, $v_{\mathbf{G}}(\mathbf{q})$ represents the Fourier coefficients of the bare Coulomb interaction, and $\epsilon^{-1}_{\mathbf{G},\mathbf{G}'}(\mathbf{q},\omega)$ are the Fourier coefficients of the inverse dielectric function,

$$\epsilon^{-1}_{\mathbf{G},\mathbf{G}'}(\mathbf{q},\omega)=\delta_{\mathbf{G},\mathbf{G}'}+\chi_{\mathbf{G},\mathbf{G}'}(\mathbf{q},\omega)v_{\mathbf{G}'}(\mathbf{q}). \quad (7)$$

Within RPA,

$$\epsilon_{\mathbf{G},\mathbf{G}'}(\mathbf{q},\omega)=\delta_{\mathbf{G},\mathbf{G}'}-\chi^0_{\mathbf{G},\mathbf{G}'}(\mathbf{q},\omega)v_{\mathbf{G}'}(\mathbf{q}), \quad (8)$$

where $\chi^0_{\mathbf{G},\mathbf{G}'}(\mathbf{q},\omega)$ are the Fourier coefficients of the density-density correlation function of noninteracting Kohn-Sham electrons (see, e.g., Ref. 28).

After introduction of the Fourier representation of Eq. (6) into Eq. (3), and in the limit that the volume of the system Ω becomes infinite, one finds the following expression for the damping rate of an electron in the state $\phi_{\mathbf{k},n_i}(\mathbf{r})$ with energy $E_{\mathbf{k},n_i}$:

$$\tau_i^{-1}=\frac{1}{\pi^2}\sum_f\int_{\mathrm{BZ}}d\mathbf{q}\sum_{\mathbf{G},\mathbf{G}'}\frac{B^*_{if}(\mathbf{q}+\mathbf{G})B_{if}(\mathbf{q}+\mathbf{G}')}{|\mathbf{q}+\mathbf{G}|^2}\times\mathrm{Im}[-\epsilon^{-1}_{\mathbf{G},\mathbf{G}'}(\mathbf{q},\omega)], \quad (9)$$

where $\omega=E_{\mathbf{k},n_i}-E_{\mathbf{k}-\mathbf{q},n_f}$ and

$$B_{if}(\mathbf{q}+\mathbf{G})=\int d\mathbf{r}\,\phi^*_{\mathbf{k},n_i}(\mathbf{r})e^{i(\mathbf{q}+\mathbf{G})\cdot\mathbf{r}}\phi_{\mathbf{k}-\mathbf{q},n_f}(\mathbf{r}). \quad (10)$$

Couplings of the wave vector $\mathbf{q}+\mathbf{G}$ to wave vectors $\mathbf{q}+\mathbf{G}'$ with $\mathbf{G}\neq\mathbf{G}'$ appear as a consequence of the existence of electron-density variations in real solids. If these terms, representing the so-called crystalline local-field effects, are neglected, one can write

$$\tau_i^{-1}=\frac{1}{\pi^2}\sum_f\int_{\mathrm{BZ}}d\mathbf{q}\sum_{\mathbf{G}}\frac{|B_{if}(\mathbf{q}+\mathbf{G})|^2}{|\mathbf{q}+\mathbf{G}|^2}\frac{\mathrm{Im}[\epsilon_{\mathbf{G},\mathbf{G}}(\mathbf{q},\omega)]}{|\epsilon_{\mathbf{G},\mathbf{G}}(\mathbf{q},\omega)|^2}. \quad (11)$$

Within RPA, Eq. (8) yields

$$\mathrm{Im}[\epsilon_{\mathbf{G},\mathbf{G}}(\mathbf{q},\omega)] = \frac{2\pi v_{\mathbf{G}}(\mathbf{q})}{\Omega} \sum_{\mathbf{k}}^{\mathrm{BZ}} \sum_{n,n'} (f_{\mathbf{k},n} - f_{\mathbf{k}+\mathbf{q},n'}) \times |\langle \phi_{\mathbf{k},n}| e^{-i(\mathbf{q}+\mathbf{G})\cdot\mathbf{r}} |\phi_{\mathbf{k}+\mathbf{q},n'}\rangle|^2 \times \delta(\omega - E_{\mathbf{k}+\mathbf{q},n'} + E_{\mathbf{k},n}). \quad (12)$$

Hence, the imaginary part of $\epsilon_{\mathbf{G},\mathbf{G}}(\mathbf{q},\omega)$ represents a measure of the number of states available for real transitions involving a given momentum and energy transfer $\mathbf{q}+\mathbf{G}$ and ω, respectively, which is renormalized by the coupling between initial and final states. The factor $|\epsilon_{\mathbf{G},\mathbf{G}}(\mathbf{q},\omega)|^{-2}$ in Eq. (11) accounts for the screening in the interaction with the probe electron. Initial and final states of the probe electron enter through the coefficients $B_{if}(\mathbf{q}+\mathbf{G})$.

If all one-electron Bloch states entering both the coefficients $B_{if}(\mathbf{q}+\mathbf{G})$ and the dielectric function $\epsilon_{\mathbf{G},\mathbf{G}'}(\mathbf{q},\omega)$ were represented by plane waves, then Eqs. (9) and (11) would exactly coincide with the *GW* scattering rate of excited electrons in a FEG, as obtained by Quinn and Ferrell[1] and by Ritchie.[2] For hot electrons with energies very near the Fermi level ($E_i \approx E_F$) this result yields, in the high-density limit ($r_s \ll 1$),[29] the well-known formula of Quinn and Ferrell,[1]

$$\tau_i^{\mathrm{QF}} = 263 r_s^{-5/2} (E_i - E_F)^{-2} \ \mathrm{eV}^2\ \mathrm{fs}. \quad (13)$$

For a detailed discussion of the range of validity of this approach, see Ref. 28.

We note that the decay τ_i^{-1} of hot electrons in periodic crystals depends on both the wave vector $\mathbf{k}$ and the band index n_i of the initial Bloch state. Nevertheless, we also define $\tau^{-1}(E)$, as the average of $\tau^{-1}(\mathbf{k},n)$ over all wave vectors and bands lying with the same energy in the irreducible wedge of the Brillouin zone (IBZ). Decay rates of hot electrons lying outside the IBZ are considered by simply using the symmetry property $\tau^{-1}(S\mathbf{k},n) = \tau^{-1}(\mathbf{k},n)$, where S represents an operator of the point group of the crystal.

For the evaluation of the polarizability $\chi^0_{\mathbf{G},\mathbf{G}'}(\mathbf{q},\omega)$ and the coefficients $B_{if}(\mathbf{q}+\mathbf{G})$, Eq. (10), we use the self-consistent LDA eigenfunctions of the one-electron Kohn-Sham Hamiltonian of DFT, which we first expand in a plane-wave basis,

$$\phi_{\mathbf{k},n}(\mathbf{r}) = \frac{1}{\sqrt{\Omega}} \sum_{\mathbf{G}} u_{\mathbf{k},n}(\mathbf{G}) e^{i(\mathbf{k}+\mathbf{G})\cdot\mathbf{r}}. \quad (14)$$

The electron-ion interaction is described by means of nonlocal, norm-conserving ionic pseudopotentials,[30,31] and the XC potential is obtained in the LDA with use of the Perdew-Zunger[32] parametrization of the XC energy of Ceperley and Alder.[33]

Well-converged results have been found with the introduction in Eq. (14) of kinetic-energy cutoffs of 12, 6, and 20 Ry for Al, Mg, and Be, respectively. In the case of Cu, all $4s^1$ and $3d^{10}$ Bloch states have been kept as valence electrons in the pseudopotential generation, and an energy cutoff as large as 75 Ry has been required, thereby keeping ~900 plane waves in the expansion of Eq. (14). Though all-electron schemes, such as the full-potential linearized augmented plane-wave method,[34] are expected to be better suited for the description of the response of localized *d* electrons, the plane-wave pseudopotential approach has already been successfully incorporated in the description of the dynamical response of copper.[35]

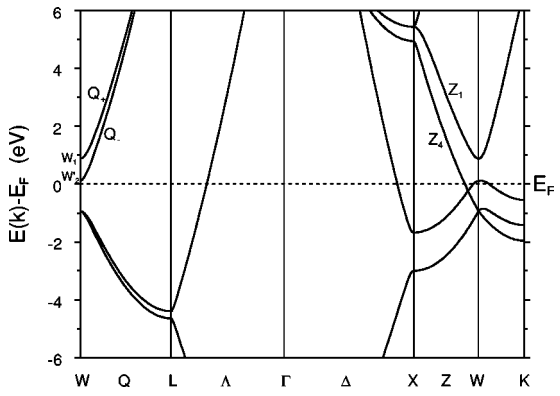

FIG. 1. Calculated band structure of Al along certain symmetry directions.

Samplings over the BZ required for the evaluation of both the dielectric matrix and the hot-electron decay rate have been performed on Monkhorst-Pack meshes:[36] 20×20×20 for Al, 24×24×10 for Mg, 24×24×16 for Be, and 16×16×16 for Cu. For hot-electron energies under study ($E - E_F \sim 0.5 - 4.0$ eV), the inclusion of up to 40 bands has been required, and the sum in Eq. (11) has been extended over 15 **G** vectors of the reciprocal lattice, the magnitude of the maximum momentum transfer $\mathbf{q}+\mathbf{G}$ being well over the upper limit of $\sim 2q_F$ (q_F is the Fermi momentum). For the evaluation of hot-electron lifetimes from Eq. (9), with full inclusion of crystalline local-field effects, dielectric matrices as large as 40×40 have been considered.

III. RESULTS AND DISCUSSION

A. Aluminum

Due to the free-electron-like nature of the energy bands of face-centered-cubic aluminum (see Fig. 1), a simple metal with no *d* bands, the impact of the band structure on the electronic excitations had been presumed for many years to be small. However, x-ray measurements[37,38] and careful first-principles calculations of the dynamical density response of this material[39,40] have shown that band-structure effects cannot be neglected. Full band-structure calculations of the electronic stopping power of Al for slow ions have shown that the energy loss is ~7% larger than that of a FEG.[41] Our present calculations indicate that actual hot-electron lifetimes in Al are ~35% smaller than those of electrons in a FEG.

Our *ab initio GW*-RPA calculation of the average lifetime $\tau(E)$ of hot electrons in Al, as obtained from Eq. (9) with full inclusion of crystalline local-field effects, is presented in Fig. 2 by solid circles. The *GW*-RPA lifetime of hot electrons in a FEG with the electron density equal to that of valence electrons in Al ($r_s = 2.07$) is exhibited in the same figure, by a solid line. Our calculations indicate that the lifetime of hot electrons in Al is, within RPA, smaller than that of electrons in a FEG with $r_s = 2.07$ by a factor of ~0.65. We have performed band-structure calculations of Eq. (9) with and without [see also Eq. (11)] the inclusion of crystalline local-field corrections, and have found that these correc-

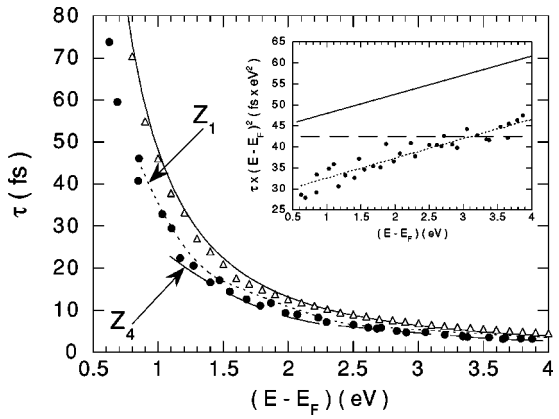

FIG. 2. Hot-electron lifetimes in Al. Solid circles represent our full *ab initio* calculation of $\tau(E)$, as obtained after averaging $\tau(\mathbf{k},n_i)$ of either Eq. (9) or Eq. (11) over wave vectors and over the band structure for each $\mathbf{k}$. The solid line represents the lifetime of hot electrons in a FEG with $r_s=2.07$, as obtained within the full *GW*-RPA. Open triangles represent the result obtained from Eq. (11) by replacing hot-electron initial and final states in $|B_{if}(\mathbf{q}+\mathbf{G}|^2$ by plane waves, but with full inclusion of the band structure in the evaluation of $\mathrm{Im}[-\epsilon^{-1}_{\mathbf{G},\mathbf{G}}(\mathbf{q},\omega)]$. Dotted and long-dashed lines represent the lifetime of hot electrons in bands Z_1 and Z_4, respectively, with the wave vector along the *WX* direction. The inset exhibits scaled lifetimes of hot electrons in Al. Solid circles and the solid line represent band-structure and FEG calculations, respectively, both within *GW*-RPA. The dashed line represents the prediction of Eq. (13).

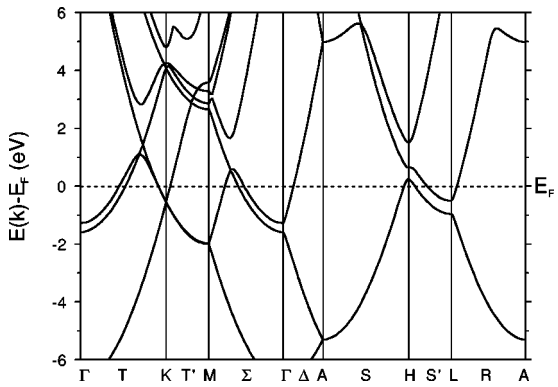

FIG. 3. Calculated band structure of Mg along certain symmetry directions.

tions are negligible for electron energies under study. This is an expected result, since Al crystal does not present strong density gradients nor special electron density directions (bondings).

In order to understand the origin of band-structure effects on hot-electron lifetimes in Al, we first focus on the role that the band structure plays in the creation of electron-hole (e-h) pairs. Hence, we evaluate hot-electron lifetimes from either Eq. (9) or Eq. (11) by replacing the electron initial and final states in $|B_{if}(\mathbf{q}+\mathbf{G})|^2$ by plane waves (plane-wave calculation). The result we obtain with full inclusion of the band structure of the crystal in the evaluation of $\mathrm{Im}\,\epsilon^{-1}_{\mathbf{G},\mathbf{G}'}(\mathbf{q},\omega)$ is represented in Fig. 2 by open triangles. Due to splitting of the band structure over the Fermi level, new channels are opened for e-h pair production, and band-structure effects tend, therefore, to decrease the lifetime of very-low-energy electrons by $\sim$5%, as in the case of slow ions.[41]

In the case of moving ions, differences between actual decay rates and those obtained in a FEG only enter through the so-called energy-loss matrix, $\mathrm{Im}[-\epsilon^{-1}_{\mathbf{G},\mathbf{G}'}(\mathbf{q},\omega)]$. However, hot-electron decay rates are also sensitive to the actual initial and final states entering the coefficients $B_{if}(\mathbf{q}+\mathbf{G})$. Differences between our full (solid circles) and plane-wave (open triangles) calculations come from this sensitivity of hot-electron initial and final states on the band structure of the crystal, showing that the splitting of the band structure over the Fermi level now plays a major role in lowering the hot-electron lifetime.

Scaled lifetimes, $\tau(E)\times(E-E_F)^2$, of hot electrons in Al, as obtained from our full band-structure calculation (solid circles) and from the FEG model with $r_s=2.07$ (solid line), are represented in the inset of Fig. 2. In the limit $E\rightarrow E_F$, the available phase space for real transitions is simply $E-E_F$, which yields the $(E-E_F)^{-2}$ quadratic scaling of very-low-electron energies in a FEG, as predicted by Eq. (13) (dashed line).[42] However, as the energy increases, momentum and energy conservation prevents the available phase space from being as large as $E-E_F$, and the lifetime of electrons in a FEG depart, therefore, from the $(E-E_F)^{-2}$ scaling. For energies under study, band-structure effects in Al are found to be nearly energy independent; hence, our calculated lifetimes are found to approximately scale as in the case of electrons in a FEG, and they slightly depart, therefore, from the $(E-E_F)^{-2}$ scaling. The agreement at $E-E_F\sim 3$ eV between actual lifetimes and those predicted by Eq. (13) is simply due to the nearly thorough compensation, at these energies, between the departure of this formula from full free-electron-gas RPA calculations and band-structure effects.

Although the energy bands of Al show an overall similarity with the fcc free-electron band structure, in the vicinity of the *W* point there are large differences between the two cases (see Fig. 1). At this point, the free-electron parabola opens an energy gap around the Fermi level and splits along the *WX* direction into two bands (Z_1 and Z_4) with energies over the Fermi level. We have calculated lifetimes of hot electrons in these bands, with the wave vector along the *WX* direction. The results of these calculations are exhibited in Fig. 2, as a function of energy, by dotted (Z_1) and long-dashed lines (Z_4). Although hot electrons in the Z_1 band have one more channel available to decay along the *WX* direction, the band gap at the *W* point around the Fermi level results in hot electrons living longer on the Z_1 than on the Z_4 band. When the hot-electron energy is well above the Fermi level ($E-E_F>4$ eV), both Z_1 and Z_4 lifetimes nearly coincide with the average values represented by solid circles. We have evaluated hot-electron lifetimes along other directions of the wave vector, and have found that differences between these results and average lifetimes are not larger than those obtained along the *WX* direction. This is in disagreement with the calculations reported by Schöne *et al.*[22] In particular, the bending of the hot-electron lifetime along the *WL* direction at $\sim$1 eV reported in Ref. 22 is not present in our calculations. The origin of this discrepancy is the crossing near the Fermi level between bands Q_+ and Q_- along the *WL* direction reported in Ref. 22. This crossing is absent in the present (see Fig. 1) and previous[30,43–45] self-consistent band-

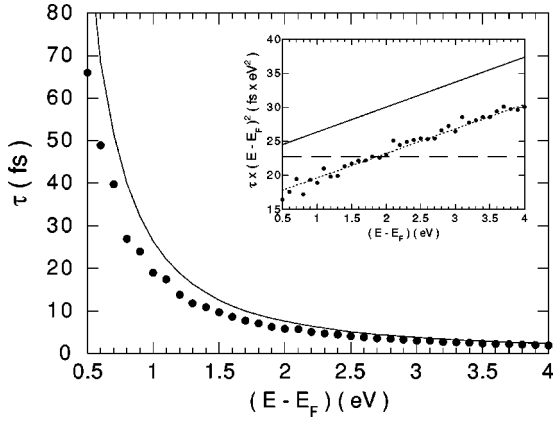

FIG. 4. Hot-electron lifetimes in Mg. As in Fig. 2 with $r_s = 2.66$.

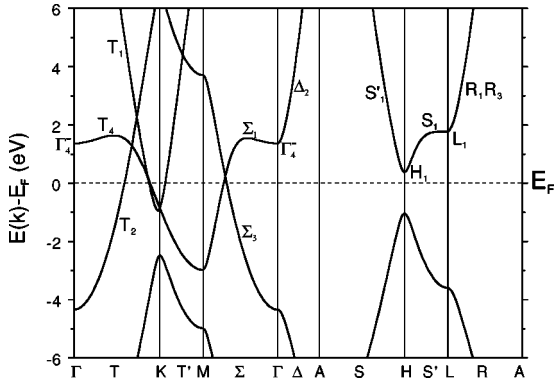

FIG. 5. Calculated band structure of Be along certain symmetry directions.

structure calculations, which all show that at the W point of the Al band structure the level W_2' is below W_1.

B. Magnesium

In Fig. 3 we show the band structure of hexagonal closed-packed (hcp) magnesium. There is a close resemblance for energies $E < E_F$ between this band structure and that of free electrons, though the free-electron parabola now splits near the Fermi level along certain symmetry directions. As a result, the energy-loss function, $\mathrm{Im}[-\epsilon^{-1}_{\mathbf{G},\mathbf{G}'}(\mathbf{q},\omega)]$, of this material is approximately well described within a free-electron model, and band-structure effects on hot-electron lifetimes enter mainly, as in the case of Al, through the sensitivity of hot-electron initial and final states on the band structure of the crystal.

Our *ab initio* calculation of the average lifetime $\tau(E)$ of hot electrons in Mg, as obtained from Eq. (9) with full inclusion of crystalline local-field effects, is presented in Fig. 4 by solid circles, together with the lifetime of hot electrons in a FEG with the electron density equal to that of valence electrons in Mg ($r_s = 2.66$). As in the case of Al, we have found that local-field corrections are negligible for electron energies under study.

Scaled lifetimes of hot electrons in Mg, as obtained from our full band-structure calculations (solid circles) and from the FEG model with $r_s = 2.66$ (solid line), are represented in the inset of Fig. 4. We note that actual lifetimes in this material scale with energy approximately as in the case of electrons in a FEG, thereby slightly deviating from the $(E - E_F)^{-2}$ scaling predicted by Eq. (13) (dashed line). Because of splitting of the band structure over the Fermi level new decay channels are opened, not present in the case of a FEG, and band-structure effects tend, therefore, to decrease the lifetime of hot electrons in Mg by a factor of ~ 0.75. Since the splitting of the band structure of Mg is not as pronounced as that of Al, the departure of actual lifetimes from those of electrons in a FEG is found to be smaller in Mg than in Al.

C. Beryllium

Among the so-called simple metals, with no d bands, beryllium presents distinctive features in that its band structure (see Fig. 5) exhibits the largest departure from free-electron behavior. Both Be and Mg have hcp crystal structure and two conduction electrons per atom. Nevertheless, the electronic structure of Be is qualitatively different from that of Mg, the Be band gaps at points Γ, H, and L being much larger than those in Mg. Also, the Be band gaps are located on both sides of the Fermi level, and the density of states (DOS) of this material falls to a sharp minimum near the Fermi level.

Our band-structure calculation of the average lifetime $\tau(E)$ of hot electrons in Be is shown in Fig. 6 by solid circles, as obtained from Eq. (9). The lifetime of hot electrons in a FEG with the electron density equal to that of valence electrons in Be ($r_s = 1.87$) is represented in the same figure by a solid line. In the inset, the corresponding scaled calculations are plotted, together with the results obtained from Eq. (13) (dashed line). It can be seen that large deviations from the FEG calculation occur for electron energies near the Fermi level ($E - E_F < 3$ eV), especially at $E - E_F \sim 1.4$ and 1.8 eV where the presence of band gaps at points Γ and L plays a key role. We note that the deep departure from free-electron behavior of the beryllium DOS near the Fermi level tends to increase the inelastic lifetime of all excited Bloch states. Furthermore, actual lifetimes strongly deviate from the $\sim (E - E_F)^{-2}$ scaling predicted within Fermi-liquid theory. This deviation comes from the contribution to the average lifetime due to Bloch states near the points Γ and L with energies close to the energy gap.

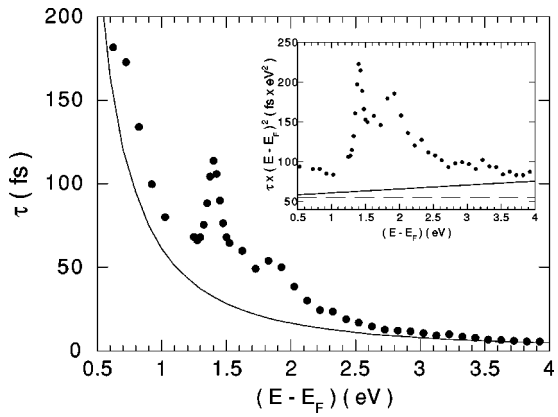

FIG. 6. Hot-electron lifetimes in Be. As in Fig. 2 with $r_s = 1.87$.

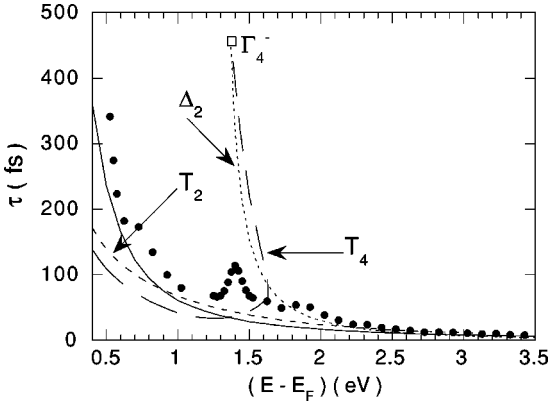

FIG. 7. Hot-electron lifetimes in Be. Solid circles and the solid line represent the same quantities as in Fig. 6. Short-dashed and long-dashed lines represent the lifetime of hot electrons in bands T_2 and T_4, respectively, with the wave vector along the ΓK direction. The dotted line represents the lifetime of hot electrons in the Δ_2 band along the ΓA direction. The open square is located at the energy of the level Γ_4^-, showing the beginning and the end of the Δ_2 and T_4 bands, respectively.

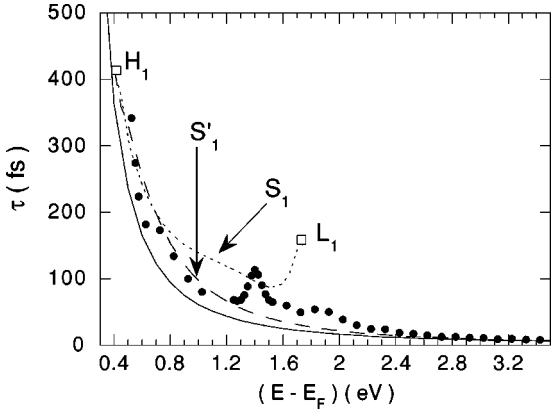

FIG. 8. Hot-electron lifetimes in Be. Solid circles and the solid line represent the same quantities as in Fig. 6. Dotted and dashed lines represent the lifetime of hot electrons in bands S_1 and S_1', respectively, with the wave vector along the LH and HA directions. Open squares are located at the energy of the levels L_1 and H_1.

At the Γ point, the free-electron parabola opens a wide energy gap around the Fermi level and splits along the ΓK and ΓM directions into two bands, T_2/T_4 and Σ_1/Σ_3, respectively. The results of our calculated lifetimes of hot electrons in bands T_2 and T_4, with the wave vector along the ΓK direction, are plotted in Fig. 7 by short-dashed and long-dashed lines, respectively. For comparison, the average lifetime of hot electrons in real beryllium and in a FEG with $r_s=1.87$ are also plotted in this figure by solid circles and by a solid line, respectively. At very-low electron energies ($E-E_F<1$ eV), interband transitions yield lifetimes of hot electrons in the T_2 band that are below those of electrons in a FEG, as in the case of Al and Mg. However, at higher energies the coupling with lower-lying flat bands becomes small, and lifetimes of electrons in this (T_2) band are found to be above the FEG prediction. Lifetimes of hot electrons in the T_4 band are also, at very-low electron energies ($E-E_F<1.4$ eV), below those of electrons in a FEG. Nevertheless, at energies of $\sim$1.4 eV the presence of the band gap at Γ yields very long lifetimes, especially at the level Γ_4^-.

We have calculated hot-electron lifetimes in bands Σ_1 and Σ_3, with the wave vector along the ΓM direction, and have found results that are similar to those obtained for electrons in bands T_2 and T_4. Calculations of the lifetime of hot electrons in the Δ_2 band, with the wave vector along the ΓA direction, are also shown in Fig. 7 (dotted line). Though this is not a flat band, the presence of the gap at the Γ point near the Fermi level results in hot electrons close to the level Γ_4^- living much longer than in the case of a FEG. The combined contribution from hot electrons in bands T_4, Σ_1, and Δ_2 is the origin of the enhanced average lifetime (solid circles) at $E-E_F\sim1.4$ eV, which corresponds to the energy of the level Γ_4^- at the Γ point.

A wide band gap is also opened at the L point, which originates the enhanced average lifetime at $E-E_F\sim1.8$ eV. Hence, we have plotted in Fig. 8 the results of our calculated lifetimes of hot electrons in the S_1 band, with the wave vector along the LH direction (dotted line), together with the average lifetime of hot electrons in real Be (solid circles) and in a FEG with $r_s=1.87$ (solid line). As in the case of hot electrons in bands T_4 and Σ_1, the presence of the band gap at the L point yields a very long average lifetime, but now at $E-E_F\sim1.8$ eV. A similar behavior is obtained near the L point for electrons in the R_1R_3 band along the LA direction, and both bands S_1 and R_1R_3 contribute to the enhanced average lifetime at $E-E_F\sim1.8$ eV. In Fig. 8 we have also represented calculations of the lifetime of hot electrons in the S_1' band along the HA direction (dashed line). At low energies ($E-E_F<2$ eV), the presence of the gap at the H point leads to hot-electron lifetimes along the HA direction that are longer than those of electrons in a FEG, but departure from free-electron behavior at the H point is not as pronounced as at the Γ or L points. At higher energies, the S_1' band shows great similarity with the corresponding hcp free-electron band, and lifetimes nearly coincide, therefore, with those obtained within the FEG model.

D. Copper

Copper, the most widely studied metal by TR-2PPE, is a noble metal with entirely filled $3d$-like bands. In Fig. 9 we show the energy bands of this fcc crystal. We see a profound difference between the band structure of Cu and that of free

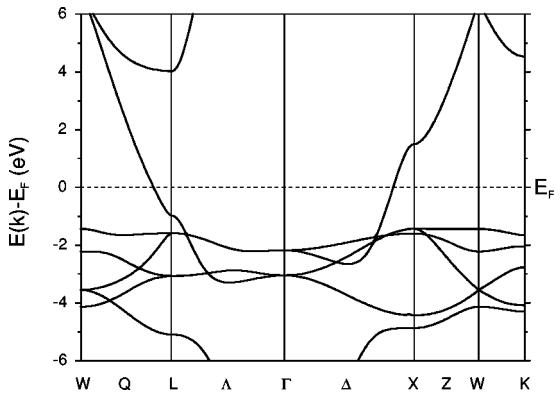

FIG. 9. Calculated band structure of Cu along certain symmetry directions.

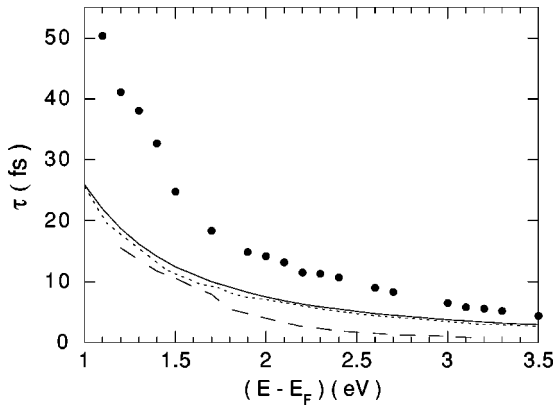

FIG. 10. Hot-electron lifetimes in Cu as in Fig. 2 with $r_s=2.67$. The dashed line represents the result of replacing all one-electron Bloch states by plane waves (FEG calculation) but keeping in Eq. (12) the actual number of states available for real transitions (Ref. 46). The dotted line represents our full *ab initio* calculation of $\tau(E)$, as obtained after averaging $\tau(\mathbf{k},n_i)$ of Eq. (9) over wave vectors and over the band structure for each $\mathbf{k}$, but with the $3d$ shell assigned to the core in the pseudopotential generation.

electrons. Slightly below the Fermi level, at $E-E_F\sim 2$ eV, we have *d* bands capable of holding 10 electrons per atom, the one remaining electron being in a free-electron-like band below and above the *d* bands. Hence, a combined description of both delocalized $4s^1$ and localized $3d^{10}$ electrons is needed to address the actual electronic response of this material. The results presented below have been found by keeping all $4s^1$ and $3d^{10}$ Bloch states as valence electrons in the pseudopotential generation.

Band-structure *GW*-RPA calculations of the average lifetime $\tau(E)$ of hot electrons in Cu are exhibited in Fig. 10 by solid circles, as obtained from Eq. (9) with full inclusion of crystalline local-field effects. The lifetime of hot electrons in a FEG with the electron density equal to that of $4s^1$ electrons in Cu ($r_s=2.67$) is represented by a solid line. These calculations indicate that the lifetime of hot electrons in Cu is, within RPA, larger than that of electrons in a FEG with $r_s=2.67$, this enhancement varying from a factor of $\sim$2.5 near the Fermi level ($E-E_F=1.0$ eV) to a factor of $\sim$1.5 for $E-E_F=3.5$ eV. In order to investigate the role that localized *d* bands play in the decay mechanism of hot electrons, we have also used an *ab initio* pseudopotential with the $3d$ shell assigned to the core. The result of this calculation, displayed in Fig. 10 by a dotted line, shows that it nearly coincides with the FEG calculation; thus, *d*-band states play a key role in the hot-electron decay.

We have performed band-structure calculations of Eq. (9) with and without [see also Eq. (11)] the inclusion of crystalline local-field corrections, and have found that these corrections are negligible for $E-E_F>1.5$ eV, while for energies very near the Fermi level, neglecting these corrections results in an overestimation of the lifetime of less than 5%. Therefore, differences between our full band-structure calculations (solid circles) and FEG calculations (solid line) come from the actual density of states (DOS) available for real excitations, localization, additional screening, and Fermi-surface topology.

First of all, we focus on the role that both DOS and coupling between Bloch states participating in the creation of *e*-*h* pairs, i.e., localization [see Eq. (12)] play in the hot-electron decay mechanism. Hence, we neglect crystalline local-field effects and present the result of evaluating hot-electron lifetimes from Eq. (11) by replacing initial and final states in $|B_{if}(\mathbf{q}+\mathbf{G})|^2$ by plane waves and the dielectric function in $|\epsilon_{\mathbf{G},\mathbf{G}}(\mathbf{q},\omega)|^{-2}$ by that of a FEG with $r_s=2.67$. If we further replaced $\mathrm{Im}[\epsilon_{\mathbf{G},\mathbf{G}}(\mathbf{q},\omega)]$ by that of a FEG, then we would obtain the FEG calculation represented by a solid line. The impact of the actual DOS below the Fermi level may be described by simply replacing the one-electron Bloch states in Eq. (12) by plane waves but keeping the actual number of states available for real excitations. The result of this calculation[46] is represented in Fig. 10 by a dashed line. This result is very close to that reported by Ogawa *et al.*,[13] though these authors approximated the FEG dielectric function in $|\epsilon_{\mathbf{G},\mathbf{G}}(\mathbf{q},\omega)|^{-2}$ within the static Thomas-Fermi model.

It is clear from Fig. 10 that the actual DOS available for real transitions yields lifetimes that are shorter than those obtained in a FEG model, especially for $E-E_F>2$ eV due to opening of the *d*-band scattering channel dominating the DOS with energies $\sim$2 eV. However, if one takes into account, within a full description of the band structure of the crystal in the evaluation of $\mathrm{Im}[\epsilon_{\mathbf{G},\mathbf{G}}(\mathbf{q},\omega)]$, the actual coupling between initial and final states avaliable for real transitions, then one obtains hot-electron lifetimes which lie, at very-low electron energies ($E-E_F<2.5$ eV), just above the FEG curve (see open circles in Fig. 1 of Ref. 21). This enhancement of the lifetime, even at energies below the opening of the *d*-band scattering channel, is due to the fact that states just below the Fermi level have a small but significant *d* component, thus being more localized than pure *sp* states.

The combined effect of DOS and localization, which enters through the imaginary part of the dielectric matrix $\mathrm{Im}[\epsilon_{\mathbf{G},\mathbf{G}'}(\mathbf{q},\omega)]$, increases the lifetime of hot electrons with energies $E-E_F<2.5$ eV (see open circles in Fig. 1 of Ref. 21). As for the departure of hot-electron initial and final states from free-electron behavior, entering through the coefficients $B_{if}(\mathbf{q}+\mathbf{G})$, we have found that it yields hot-electron lifetimes that are strongly directional dependent, with Fermi surface shape effects tending to decrease the average inelastic lifetime of very-low-energy electrons ($E-E_F<2.5$ eV) (see Ref. 21). Furthermore, the combined effect of DOS and localization, on the one hand, and Fermi-surface shape effects, on the other hand, nearly compensate. Consequently, large differences between hot-electron lifetimes in real Cu and in a FEG with $r_s=2.67$, are mainly due to a major contribution from *d* electrons participating in the screening of electron-electron interactions, which is accounted for by the factor $|\epsilon_{\mathbf{G},\mathbf{G}}(\mathbf{q},\omega)|^{-2}$ in Eq. (11).

The Fermi surface of Cu is greatly flattened in certain regions, showing a pronounced neck in the direction ΓL. Thus, the isotropy of hot-electron lifetimes in a FEG disappears in this material. While flattening of the Fermi surface along the ΓK direction is found to decrease the hot-electron lifetime by a factor that varies from $\sim$15% near the Fermi level ($E-E_F=1$ eV) to $\sim$5% for $E-E_F=3.5$ eV (see also Ref. 47), the lifetime of hot electrons with the wave vector along the necks of the Fermi surface, in the ΓL direction, is

found to be much longer than the average lifetime. We have calculated hot-electron lifetimes in the Λ_1 band, with the wave vector along the ΓL direction, and have found the lifetime of hot electrons at the L_1 level with $E-E_F=4.2$ eV to be longer than the average lifetime at this energy by $\sim 80\%$.

A comparison between our calculated hot-electron lifetimes in Cu and those determined from most recent TR-2PPE experiments was presented in Ref. 21. At $E-E_F<2$ eV, our calculations are close to lifetimes recently measured by Knoesel *et al.* in the very-low energy range.[16] At larger electron energies, good agreement between our band-structure calculations and experiment is obtained for Cu(110),[13] the only surface with no band gap in the $\mathbf{k}_\parallel=0$ direction.

IV. CONCLUSIONS

We have presented full *GW*-RPA band-structure calculations of the inelastic lifetime of hot electrons in Al, Mg, Be, and Cu, and have demonstrated that decay rates of low-energy excited electrons strongly depend on the details of the electronic band structure. Though the dependence of hot-electron lifetimes in Al and Mg on the direction of the wave vector has been found not to be large, in the case of Be and Cu hot-electron lifetimes have been found to be strongly directional dependent. Furthermore, very long lifetimes at certain points of the BZ in Be yield average lifetimes in this material that strongly deviate from the $\sim(E-E_F)^{-2}$ scaling predicted within Fermi-liquid theory.

As far as band-structure effects on hot-electron energies and wave functions are concerned, we have found that both splitting of the band structure and the presence of band gaps over the Fermi level play an important role in the e-e decay mechanism. In Al and Mg, splitting of the band structure is found to yield electron lifetimes that are smaller than those of electrons in a FEG. On the other hand, large deviations of the band structure of Be along certain symmetry directions from the free-electron model near the Fermi level result in a strong directional dependence of hot-electron lifetimes in this material.

As for the presence of band-structure effects on the creation of e-h pairs, there are contributions from the actual DOS available for real transitions, from localization, i.e., the actual coupling between electron and hole states, and from screening. The combined effect of DOS and localization is found not to be large, even in the case of a noble metal like Cu with d bands. However, large differences between hot-electron lifetimes in Cu and in a FEG with the electron density equal to that of valence $(4s^1)$ electrons are found to be due to a major contribution from d electrons participating in the screening of e-e interactions.

Crystalline local-field corrections in these materials have been found to be small for hot-electron energies under study.

ACKNOWLEDGMENTS

We would like to thank A. G. Eguiluz for stimulating discussions. We also acknowledge partial support by the University of the Basque Country, the Basque Hezkuntza, Unibertistate eta Ikerketa Saila, and the Spanish Ministerio de Educación y Cultura.

[1] J. J. Quinn and R. A. Ferrell, Phys. Rev. **112**, 812 (1958).
[2] R. H. Ritchie, Phys. Rev. **114**, 644 (1959).
[3] J. J. Quinn, Phys. Rev. **126**, 1453 (1962).
[4] R. H. Ritchie and J. C. Ashley, J. Phys. Chem. Solids **26**, 1689 (1965).
[5] L. Kleinman, Phys. Rev. B **3**, 2982 (1971).
[6] J. C. Shelton, Surf. Sci. **44**, 305 (1974).
[7] D. R. Penn, Phys. Rev. B **13**, 5248 (1976).
[8] C. J. Tung, J. C. Ashley, and R. H. Ritchie, Surf. Sci. **81**, 427 (1979).
[9] D. R. Penn, Phys. Rev. B **22**, 2677 (1980).
[10] D. R. Penn, Phys. Rev. B **35**, 482 (1987).
[11] C. A. Schmutenmaer, M. Aeschlimann, H. E. Elsayed-Ali, R. J. D. Miller, D. A. Mantell, J. Cao, and Y. Gao, Phys. Rev. B **50**, 8957 (1994).
[12] T. Hertel, E. Knoesel, M. Wolf, and G. Ertl, Phys. Rev. Lett. **76**, 535 (1996).
[13] S. Ogawa, H. Nagano, and H. Petek, Phys. Rev. B **55**, 1 (1997).
[14] J. Cao, Y. Gao, R. J. D. Miller, H. E. Elsayed-Ali, and D. A. Mantell, Phys. Rev. B **56**, 1099 (1997).
[15] M. Aeschlimann, M. Bauer, S. Pawlik, W. Weber, R. Burgermeister, D. Oberli, and H. C. Siegmann, Phys. Rev. Lett. **79**, 5158 (1997).
[16] E. Knoesel, A. Hotzel, and M. Wolf, Phys. Rev. B **57**, 12 812 (1998).
[17] A. Goldmann, R. Matzdorf, and F. Theilmann, Surf. Sci. **414**, L932 (1998).
[18] J. Cao, Y. Gao, H. E. Elsayed-Ali, R. J. D. Miller, and D. A. Mantell, Phys. Rev. B **58**, 10 948 (1998).
[19] M. Bauer, S. Pawlik, and M. Aeschlimann, Proc. SPIE **3272**, 201 (1998).
[20] H. Petek and S. Ogawa, Prog. Surf. Sci. **56**, 239 (1998).
[21] I. Campillo, J. M. Pitarke, A. Rubio, E. Zarate, and P. M. Echenique, Phys. Rev. Lett. **83**, 2230 (1999).
[22] W.-D. Schöne, R. Keyling, M. Bandić, and W. Ekardt, Phys. Rev. B **60**, 8616 (1999).
[23] P. Hohenberg and W. Kohn, Phys. Rev. **136**, B864 (1964); W. Kohn and L. Sham, Phys. Rev. **140**, A1133 (1965).
[24] A. L. Fetter and J. D. Walecka, *Quantum Theory of Many-Particle Systems* (McGraw-Hill, New York, 1971).
[25] L. Hedin and S. Lundqvist, Solid State Phys. **23**, 1 (1969).
[26] E. Runge and E. K. U. Gross, Phys. Rev. Lett. **52**, 997 (1984).
[27] M. Petersilka, U. J. Gossmann, and E. K. U. Gross, Phys. Rev. Lett. **76**, 1212 (1996).
[28] P. M. Echenique, J. M. Pitarke, E. V. Chulkov, and A. Rubio, Chem. Phys. **251**, 1 (2000).
[29] The so-called electron-density parameter r_s is defined by the relation $1/n_0=(4/3)\pi r_s^3$, n_0 being the average electron density.
[30] V. M. Silkin, E. V. Chulkov, I. Yu. Sklyadneva, and V. E. Panin, Izv. Vuzov. Fiz. **9**, 56 (1984) [Sov. Phys. J. **27**, 762 (1984)]; E. V. Chulkov, V. M. Silkin, and E. N. Shirykalov, Fiz. Met. Metalloved. **64**, 213 (1987) [Phys. Met. Metallogr. **64**, 1 (1987)].
[31] N. Troullier and J. L. Martins, Phys. Rev. B **43**, 1993 (1991).

[32] J. P. Perdew and A. Zunger, Phys. Rev. B **23**, 5048 (1981).
[33] D. M. Ceperley and B. J. Alder, Phys. Rev. Lett. **45**, 1196 (1980).
[34] D. J. Singh, *Plane Waves, Pseudopotentials, and the LAPW Method* (Kluwer, Boston, 1994).
[35] I. Campillo, A. Rubio, and J. M. Pitarke, Phys. Rev. B **59**, 12 188 (1999).
[36] H. J. Monkhorst and J. D. Pack, Phys. Rev. B **13**, 5188 (1976).
[37] P. M. Platzman, E. D. Isaacs, H. Williams, P. Zschack, and G. E. Ice, Phys. Rev. B **46**, 12 943 (1992).
[38] W. Schulke, H. Schulte-Schrepping, and J. R. Schmitz, Phys. Rev. B **47**, 12 426 (1993).
[39] A. Fleszar, A. A. Quong, and A. G. Eguiluz, Phys. Rev. Lett. **74**, 590 (1995).
[40] B. C. Larson, J. Z. Tischler, E. D. Isaacs, P. Zschack, A. Fleszar, and A. G. Eguiluz, Phys. Rev. Lett. **77**, 1346 (1997).
[41] I. Campillo, J. M. Pitarke, and A. G. Eguiluz, Phys. Rev. B **58**, 10 307 (1998).
[42] The prediction of Eq. (13) (dashed line in the inset of Figs. 2, 4, 6, and 10) would coincide, as $E \rightarrow E_F$, with the full RPA free-electron gas calculation only in the high-density ($r_s \rightarrow 0$) limit.
[43] S. P. Singhal and J. Callaway, Phys. Rev. B **16**, 1744 (1977).
[44] F. Szumulowicz and B. Segall, Phys. Rev. B **21**, 5628 (1980).
[45] D. A. Papaconstantopoulos, *Handbook of the Band Structure of Elemental Solids* (Plenum Press, New York, 1986).
[46] We have followed Ogawa *et al.* (Ref. 13) to take the electron-density parameter r_s in the evaluation of $|\epsilon_{\mathbf{G},\mathbf{G}}(\mathbf{q},\omega)|^{-2}$ from the actual DOS at the Fermi level.
[47] S. L. Adler, Phys. Rev. **130**, 1654 (1963).